

Minimum Structural Sensor Placement for Switched Linear Time-Invariant Systems and Unknown Inputs

Emily A. Reed*, Guilherme Ramos*, Paul Bogdan, Sérgio Pequito

July 29, 2021

Abstract

In this paper, we study the structural state and input observability of continuous-time switched linear time-invariant systems and unknown inputs. First, we provide necessary and sufficient conditions for their structural state and input observability that can be efficiently verified in $O((m(n+p))^2)$, where n is the number of state variables, p is the number of unknown inputs, and m is the number of modes. Moreover, we address the minimum sensor placement problem for these systems by adopting a feed-forward analysis and by providing an algorithm with a computational complexity of $O((m(n+p) + \alpha)^{2.373})$, where α is the number of target strongly connected components of the system's digraph representation. Lastly, we explore different assumptions on both the system and unknown inputs (latent space) dynamics that add more structure to the problem, and thereby, enable us to render algorithms with lower computational complexity, which are suitable for implementation in large-scale systems.

1 Introduction

Scientists and engineers model systems by describing the nature of their dynamics and the environment in which they interact. One powerful tool to model complex switching dynamics is to adopt a switched linear time-invariant framework. This model assumes that the system under scrutiny transitions between different (yet known) linear time-invariant dynamics, where such transitions are discrete in nature and are captured by a switching signal for which the sequence of the switches may not be known *a priori*. Examples of such systems include the power electric grid [9], where the change in dynamics may be dictated by a faulty transmission line [24, 23], or a multi-agent system [27, 26], where the dynamics may change due to a loss in communication among agents.

However, modeling scenarios often neglect the fact that the interaction of a dynamical system with its environment introduces errors. We can describe these external environmental errors by unknown inputs entering into the dynamical system. For instance, in the power grid, the generated power and/or the customer demand behave as unknown inputs. Similarly, in multi-agent robotic systems, particularly in surface vehicles, friction behaves as an unknown input, whereas in the context of unmanned aerial vehicles, airflow or ocean currents act as unknown inputs. An alternate scenario is in networked systems where the unknown input is due to the interconnections with the remaining hidden network [12, 2, 8, 30, 10, 11]. As is evident in the previously mentioned examples, in control engineering, a recurrent practice is that of modeling the unknown inputs in a latent space that can capture the main features of the incoming signal but does not model the system from which the unknown input originates.

To monitor such switched linear time-invariant systems under unknown inputs requires us to assess both the state and the inputs by guaranteeing that the system is state and input observable [29]. Often, however, we cannot accurately know the parameters of the system. Moreover, if the parameters are known, the study of controllability and/or observability properties leads to NP-hard problems [25]. Hence, we assume that only the structure of the system is

*Both authors contributed equally. E. Reed is with the Ming Hsieh Electrical and Computer Engineering Department at the University of Southern California, USA. G. Ramos is with the Department of Electrical and Computer Engineering, Faculty of Engineering, University of Porto, Portugal. P. Bogdan is a faculty member at the University of Southern California in the Ming Hsieh Electrical and Computer Engineering Department. S. Pequito is a faculty member at the Delft University of Technology in the Delft Center for Systems and Control. This work was supported in part by FCT project POCI-01-0145-FEDER-031411-HARMONY, National Science Foundation GRFP DGE-1842487, Career Award CPS/CNS-1453860, CCF-1837131, MCB-1936775, CNS-1932620, CMMI-1936624, CMMI 1936578, the University of Southern California Annenberg Fellowship, USC WiSE Top-Off Fellowship, the DARPA Young Faculty Award and DARPA Director Award N66001-17-1-4044. The views, opinions, and/or findings contained in this article are those of the authors and should not be interpreted as representing the official views or policies, either expressed or implied by the Defense Advanced Research Projects Agency, the Department of Defense or the National Science Foundation.

known meaning that a system parameter is either zero or could take on any real scalar value [22]. In this context, we can rely on the notion of structural state and input observability that yields state and input observability for almost all system parameterizations.

Previous work has provided the necessary and sufficient conditions to ensure *structural* state and input observability for discrete-time systems under unknown inputs [28]. Nonetheless, the counterpart for continuous-time switched linear-time invariant systems under unknown inputs were only studied in [4] and [5, 3]. In particular, [4, 3] considers the graph-theoretic necessary and sufficient conditions for generic discrete mode observability of a continuous-time switched linear system with unknown inputs and proposed a computational method to verify such conditions with a complexity of $O(n^6)$, where n is the number of states. The works of [5, 3] present sufficient conditions for the generic observability of the discrete mode of continuous-time switched linear systems with unknown inputs and find an exhaustive location set to place sensors when these conditions are not satisfied with a computational complexity of $O(n^4)$. However, none of these works considered the minimum number of required sensors and their placement to guarantee structural state and input observability as we consider in this work. This problem is important in designing control schemes for large scale systems and is often referred to as the *minimum sensor placement*. While this problem has been studied for a variety of systems [19], to the best of the authors' knowledge, it has not been studied in the context of continuous-time switched linear time-invariant systems under unknown inputs.

The main contributions of this manuscript are as follows. We first provide necessary and sufficient conditions for structural state and input observability of continuous-time switched linear-time invariant systems under unknown inputs. Moreover, we can verify these conditions in $O((m(n+p))^2)$, where n is the number of state variables, p is the number of unknown inputs, and m is the number of modes. Furthermore, we address the minimum sensor placement for these systems using a feed-forward analysis and an algorithm with a computational complexity of $O((m(n+p)+\alpha)^{2.373})$, where the $n \times n$ matrix multiplication algorithm with best asymptotic complexity runs in $O(n^\zeta)$, with $\zeta \approx 2.3728596$ [1], and where α is the number of target strongly connected components of the system's digraph representation. We explore different assumptions on both the system and unknown input (latent space) dynamics to obtain more structure that enables us to provide new algorithms with lower computational complexity suitable to deal with large-scale systems. Finally, we present a real-world example from power systems to illustrate our results.

We structure the remainder of our paper as follows. Section 2 provides the addressed problem formulation. Section 3 presents the main results including two graph-theoretic conditions for structural state and input observability for switched linear time-invariant systems with unknown inputs as well as an algorithm that determines the minimum set of state and input variables for ensuring structural state and input observability. Section 4 discusses several classes of switched linear time-invariant systems for which we can find a solution with a better computational complexity. Section 5 provides a real-world example from power systems to illustrate our results. Finally, Section 6 concludes the paper and points out new directions for future research.

2 Problem statement

In this paper, we consider a continuous-time switched linear time-invariant (LTI) system with (unknown) inputs that can be described as follows:

$$\dot{x}(t) = A_{\sigma(t)}x(t) + F_{\sigma(t)}d(t), \quad (1a)$$

$$\dot{d}(t) = Q_{\sigma(t)}d(t), \quad (1b)$$

$$y(t) = C_{\sigma(t)}x(t) + D_{\sigma(t)}d(t), \quad (1c)$$

where $x(t) \in \mathbb{R}^n$ is the state, $d(t) \in \mathbb{R}^p$ represents the unknown inputs, $y(t) \in \mathbb{R}^n$ is the output, and $\sigma(t) : [0, \infty) \rightarrow \mathbb{M} \equiv \{1, \dots, m\}$ is the unknown switching signal. System (1) contains m possible known subsystems also known as *modes*, which we denote by the tuple $(A_k, F_k, Q_k, C_k, D_k)$, where $\sigma(t) = k \in \mathbb{M}$. Lastly, we implicitly assume that the dwell time of each mode is greater than 0.

In what follows, we seek to assess and determine the minimum sensor placement that ensures state and input observability for the continuous-time switched LTI system with unknown inputs in (1).

Definition 1 (State and Input Observability

[18]). *The switched LTI system described by $(A_{\sigma(t)}, F_{\sigma(t)}, Q_{\sigma(t)}, C_{\sigma(t)}, D_{\sigma(t)}, \sigma(t); T_f)$ is said to be state and input observable for a time horizon T_f if and only if the initial state $x(t_0)$ and the unknown inputs $d(t)$ where $t \in [t_0, T_f]$ can be uniquely determined, given $(A_{\sigma(t)}, F_{\sigma(t)}, Q_{\sigma(t)}, C_{\sigma(t)}, D_{\sigma(t)}, \sigma(t); T_f)$ and measurements $y(t)$ ($t_0 \leq t \leq T_f$). \circ*

In this paper, we focus on the sensor placement problem. For the sake of simplicity, we assume that the measurements take the following form

$$y(t) = Cx(t) + Dd(t). \quad (1c')$$

Simply speaking, we assume that the output and feed-forward matrices are the same across all modes. Notice that this assumption can be waived as we discuss in the following Remark 2.

Remark 2. We can consider a fixed set of measurements represented by C and D without loss of generality since taking the union of the measurements made in different modes, represented by $C_{\sigma(t)}$ and $D_{\sigma(t)}$, will result in the total set represented by C and D . \diamond

We assume that each sensor is dedicated, meaning that each sensor can measure only one state or only one input. Considering an arbitrary set of sensors would lead to an NP-hard problem as this is the case for the linear time-invariant systems [19]. We state this formally in the following assumption.

A1 The output matrix and feed-forward matrix are written as $C = \mathbb{I}_n^{\mathcal{J}_x}$ and $D = \mathbb{I}_p^{\mathcal{J}_d}$, where $\mathbb{I}_n^{\mathcal{J}_x}$ is a matrix where its rows are composed of canonical identity matrix rows that are each multiplied with any arbitrary value. These canonical rows are indexed by $\mathcal{J}_x = \{1, \dots, n\}$. Similarly, $\mathbb{I}_p^{\mathcal{J}_d}$ is a matrix where its rows are composed of canonical identity matrix rows that are each multiplied with any arbitrary value. These canonical vectors are indexed by $\mathcal{J}_d = \{1, \dots, p\}$.

Due to uncertainty in the system's parameters, we consider a structural systems framework [22]. We introduce the following definition for a structural matrix.

Definition 3. (Structural Matrix) A matrix $\bar{M} \in \{0, \star\}^{m_1 \times m_2}$ is referred to as a structural matrix if $\bar{M}_{ij} = 0$, then $M_{ij} = 0$, and if $\bar{M}_{ij} = \star$, then $M_{ij} \in \mathbb{R}$, so M_{ij} is any arbitrary real number and M_{ij} is assumed to be independent of $M_{i'j'}$ for all i, j, i', j' such that $i \neq i'$ and $j \neq j'$.

With this notion in mind, we next define structural state and input observability for the switched LTI system with unknown inputs in (1).

Definition 4. (Structural State and Input Observability) The switched LTI system with unknown inputs described by the structural matrices

$(\bar{A}_{\sigma(t)}, \bar{F}_{\sigma(t)}, \bar{Q}_{\sigma(t)}, \bar{C}_{\sigma(t)}, \bar{D}_{\sigma(t)}, \sigma(t); T_f)$ is said to be structurally state and input observable for a time horizon T_f if and only if there exists a system described by $(A_{\sigma(t)}, F_{\sigma(t)}, Q_{\sigma(t)}, C_{\sigma(t)}, D_{\sigma(t)}, \sigma(t); T_f)$ that is state and input observable and satisfies the structural pattern imposed by the structural matrices $(\bar{A}_{\sigma(t)}, \bar{F}_{\sigma(t)}, \bar{Q}_{\sigma(t)}, \bar{C}_{\sigma(t)}, \bar{D}_{\sigma(t)})$. \circ

Subsequently, the problem statement we seek to address in this paper is as follows: given $\bar{A}_{\sigma(t)}, \bar{F}_{\sigma(t)}, \bar{Q}_{\sigma(t)}$, which are the known structural matrices of system in (1a) and (1b), and time horizon T_f , we aim to find the minimum set of states \mathcal{J}_x and inputs \mathcal{J}_d that need to be measured to ensure structural state and input observability. We present this formally as

$$\begin{aligned} \min_{\substack{\mathcal{J}_x \subseteq \{1, \dots, n\} \\ \mathcal{J}_d \subseteq \{1, \dots, p\}}} & |\mathcal{J}_x| + |\mathcal{J}_d| \\ \text{s.t.} & (\bar{A}_{\sigma(t)}, \bar{F}_{\sigma(t)}, \bar{Q}_{\sigma(t)}, \mathbb{I}_n^{\mathcal{J}_x}, \mathbb{I}_p^{\mathcal{J}_d}, \sigma(t); T_f) \\ & \text{is struct. state and input observable.} \end{aligned} \quad (\mathcal{P}_1)$$

For the sake of clarity, we assume that the matrix $\bar{F}_{\sigma(t)}$ does not have zero columns as this would correspond to having disturbances that do not affect the dynamics of the system.

3 Minimum Structural Sensor Placement for Switched LTI Systems with Unknown Inputs

In this section, we proceed as follows. First, we provide necessary and sufficient conditions for the feasibility of the optimization problem \mathcal{P}_1 . Second, we characterize the minimal solution of problem \mathcal{P}_1 . Next, we develop an algorithm to obtain a solution to \mathcal{P}_1 , and we assess its computational complexity. Lastly, we provide a discussion about the trade-offs between the assumptions on the dynamics and the algorithms used to solve the proposed problem.

We start by introducing the notion of *generic rank*, which allows us to provide conditions for structural state and input observability of continuous-time switched LTI systems with unknown inputs.

Definition 5. (*Generic rank*): The generic rank (*g-rank*) of an $n_1 \times n_2$ structural matrix \bar{M} is

$$g - \text{rank}(\bar{M}) = \max_{M \in [\bar{M}]} \text{rank}(M),$$

where $[\bar{M}] = \{M \in \mathbb{R}^{n_1 \times n_2} : M_{i,j} = 0 \text{ if } \bar{M}_{i,j} = 0\}$. ◦

Next, we introduce several graph-theoretical and algebraic definitions required for defining the conditions for state and input observability of switched LTI systems with unknown inputs.

A *directed graph* associated with any structural system matrix \bar{M} is constructed in the following manner. A directed graph is written as $\mathcal{G}(\bar{M}) = (\mathcal{V}, \mathcal{E})$, where \mathcal{V} denotes the set of vertices (or nodes) such that $\mathcal{V} = \mathcal{M}_x$, and \mathcal{E} denotes the (directed) edges between the vertices in the graph such that $\mathcal{E} = \mathcal{E}_{\mathcal{M}_x, \mathcal{M}_x} = \{(m_j, m_i) : \bar{M}(i, j) \neq 0\}$. For a specific time t' such that $\sigma(t') = k$, we associate the system in (1a) and (1b) with a system digraph $\mathcal{G} \equiv \mathcal{G}(\bar{A}_k, \bar{F}_k, \bar{Q}_k, \mathbb{I}_n^{\mathcal{J}_x}, \mathbb{I}_p^{\mathcal{J}_a}) = (\mathcal{V}, \mathcal{E}^k)$, where $\mathcal{V} = \mathcal{X} \cup \mathcal{D} \cup \mathcal{Y}$, $\mathcal{X} = \{x_1, \dots, x_n\}$, $\mathcal{D} = \{d_1, \dots, d_p\}$, and $\mathcal{Y} = \{y_1, \dots, y_n\}$ are the state, unknown input, and output vertices, respectively. Furthermore, we have that $\mathcal{E}^k = \mathcal{E}_{\mathcal{X}, \mathcal{X}}^k \cup \mathcal{E}_{\mathcal{D}, \mathcal{X}}^k \cup \mathcal{E}_{\mathcal{D}, \mathcal{D}}^k \cup \mathcal{E}_{\mathcal{X}, \mathcal{Y}} \cup \mathcal{E}_{\mathcal{D}, \mathcal{Y}}$, where $\mathcal{E}_{\mathcal{X}, \mathcal{X}}^k = \{(x_j, x_i) : \bar{A}_k(i, j) \neq 0\}$, $\mathcal{E}_{\mathcal{D}, \mathcal{X}}^k = \{(d_j, x_i) : \bar{F}_k \neq 0\}$, $\mathcal{E}_{\mathcal{D}, \mathcal{D}}^k = \{(d_j, d_i) : \bar{Q}_k \neq 0\}$, $\mathcal{E}_{\mathcal{X}, \mathcal{Y}} = \{(x_j, y_i) : \mathbb{I}_n^{\mathcal{J}_x}(i, j) \neq 0\}$, and $\mathcal{E}_{\mathcal{D}, \mathcal{Y}} = \{(d_j, y_i) : \mathbb{I}_p^{\mathcal{J}_a}(i, j) \neq 0\}$ are the state, input, and output edges, respectively.

Next, we introduce a mathematical operator, which plays a key role in presenting the conditions for structural state and input observability of switched LTI systems with unknown inputs.

Definition 6. (*Union of structural matrices*) The mathematical operator \vee is an entry-wise operation such that a structural matrix $\bar{A} = \bigvee_{k=1}^m \bar{A}_k = \bar{A}_1 \vee \bar{A}_2 \vee \dots \vee \bar{A}_m$ has a non-zero entry at (i, j) if at least one of the matrices \bar{A}_k has a non-zero entry in that same location (i, j) , and $\bar{A}(i, j) = 0$, otherwise. ◦

With this definition, we introduce the directed graphs $\mathcal{G}(\bigvee_{k=1}^m \bar{A}'_k)$ and $\mathcal{G}(\bigvee_{k=1}^m \bar{A}'_k, \bar{C}')$. More specifically, $\mathcal{G}(\bigvee_{k=1}^m \bar{A}'_k) = (\mathcal{X}', \mathcal{E}_{\mathcal{X}', \mathcal{X}'})$ where $\mathcal{E}_{\mathcal{X}', \mathcal{X}'} = \{(x'_j, x'_i) : \bigvee_{k=1}^m \bar{A}'_{k,i,j} \neq 0\}$. In addition, $\mathcal{G}(\bigvee_{k=1}^m \bar{A}'_k, \bar{C}') = (\mathcal{V}, \mathcal{E})$ where $\mathcal{V} = \mathcal{X}' \cup \mathcal{Y}'$ and $\mathcal{E} = \mathcal{E}_{\mathcal{X}', \mathcal{X}'} \cup \mathcal{E}_{\mathcal{X}', \mathcal{Y}'}$ such that $\mathcal{E}_{\mathcal{X}', \mathcal{X}'} = \{(x'_j, x'_i) : \bigvee_{k=1}^m \bar{A}'_{k,i,j} \neq 0\}$ and $\mathcal{E}_{\mathcal{X}', \mathcal{Y}'} = \{(x'_j, y'_i) : \bar{C}'_{i,j} \neq 0\}$. We next introduce the necessary and sufficient conditions for structural state and input observability for continuous-time switched LTI systems with unknown inputs.

Theorem 7 (Necessary and sufficient conditions for structural state and input observability). A *continuous-time switched LTI system with unknown inputs* in (1a), (1b), and (1c') is *structurally state and input observable if and only if the next two conditions hold*:

- (i) $\mathcal{G}\left(\bigvee_{k=1}^m \bar{A}'_k, \bar{C}'\right)$ has all state vertices that access at least one output vertex;
- (ii) $g\text{-rank}([\bar{A}'_1; \dots; \bar{A}'_m; \bar{C}']) = n + p$,

where, for $k \in \mathbb{M}$ and the matrices \bar{A}'_k and \bar{C}' are defined as $\bar{A}'_k = \begin{bmatrix} \bar{Q}_k & 0 \\ \bar{F}_k & \bar{A}_k \end{bmatrix}$ and $\bar{C}' = [\bar{D} \ \bar{c}]$. ◦

Remark 8. Consider a switching signal that ensures the structural observability of the switched linear continuous-time systems. The order of transitions of system modes does not influence its structural observability. This property comes from the fact that:

- the “ \vee ” operation, in condition (i) Theorem 7, is commutative;
- a permutation of the matrices, in condition (ii) Theorem 7, yields the same *g-rank*. ◊

Next, we define a few other important graph-theoretic concepts. A *bipartite graph* denoted as \mathcal{B} associates a matrix M of dimension $n_1 \times n_2$ to two vertex sets $\mathcal{V}_r = \{1, \dots, n_1\}$ and $\mathcal{V}_c = \{1, \dots, n_2\}$, which are the set of row and column vertices, respectively. The connections in the matrix M relate to the connections between vertex sets \mathcal{V}_r and \mathcal{V}_c by an edge set $\mathcal{E}_{\mathcal{V}_c, \mathcal{V}_r} = \{(v_{c_j}, v_{r_i}) : M_{ij} \neq 0\}$ thereby allowing the bipartite graph of matrix M to be written as $\mathcal{B}(\mathcal{V}_c, \mathcal{V}_r, \mathcal{E}_{\mathcal{V}_c, \mathcal{V}_r})$. A *matching* is a collection of edges where the beginning vertex is different from the ending vertex for all edges in the set and there are no two edges in the set that have any of the same vertices. A *maximum matching* is the matching that has the maximum number of edges among all possible matchings. A *weighted bipartite graph* of a matrix M , denoted as $\mathcal{B}(\mathcal{V}_c, \mathcal{V}_r, \mathcal{E}_{\mathcal{V}_c, \mathcal{V}_r}, w)$, has weights $w : \mathcal{E}_{\mathcal{V}_c, \mathcal{V}_r} \rightarrow \mathbb{R}$ associated with the edges in the bipartite graph. Finding the maximum matching such that the sum of the weights is minimized in the weighted bipartite graph is called the *minimum weight maximum matching* (MWMM).

Now, we must introduce the notions of a strongly connected component and non-accessible states. Let $\mathbb{Z}_{\geq 0}$ denote the set of non-negative integers. First, we define a *path* of size $l \in \mathbb{Z}_{\geq 0}$ as a sequence of vertices, $p_s = (v_1, v_2, \dots, v_l)$, where the vertices do not repeat, $v_i \neq v_j$ for $i \neq j$, and (v_i, v_{i+1}) is an edge of the directed graph for $i = 1, \dots, l-1$. A *subgraph* denoted by $\mathcal{G}(\mathcal{V}', \mathcal{E}')$ is a subset of vertices $\mathcal{V}' \subset \mathcal{V}$ and its corresponding edges $\mathcal{E}' \subset \mathcal{E}$ of a particular graph $\mathcal{G}(\mathcal{V}, \mathcal{E})$. A *connected component* is any subgraph with paths that connect any two vertices in the subgraph. A connected component is said to be a *strongly connected component* (SCC) if the subgraph is maximal meaning there is no other subgraph that contains the maximal subgraph. A *sink SCC* is a strongly connected component that is connected to an output vertex. A *source SCC* is a strongly connected component that is connected to an input vertex. A *target-SCC* is a strongly connected component that does not have any outgoing edges. We note that every digraph can be represented as a directed acyclic graph (DAG), where each node in the DAG represents an SCC in the digraph. Finally, a *non-accessible state* is one that does not have a path to an output vertex (either measuring a state or input).

We present graph-theoretic conditions for structural state and input observability of continuous-time switched LTI systems with unknown inputs.

Corollary 9. *A switched LTI continuous-time system (1) is structurally observable if and only if the next two conditions hold:*

- (i) *there exists an edge from one state variable of each target-SCC of $\mathcal{G}(\bigvee_{k=1}^m \bar{A}'_k)$ to an output variable of $\mathcal{G}(\bigvee_{k=1}^m \bar{A}'_k, \bar{C}')$;*
- (ii) *$\mathcal{B}([\bar{A}'_1; \dots; \bar{A}'_m; \bar{C}'])$ has a maximum matching of size $n+p$;*

where, for $k \in \mathbb{M}$, the matrices \bar{A}'_k and \bar{C}' are defined as $\bar{A}'_k = \begin{bmatrix} \bar{Q}_k & \mathbf{0} \\ \bar{F}_k & \bar{A}_k \end{bmatrix}$ and $\bar{C}' = [\bar{D} \ \bar{c}]$. ◦

In the following remark, we outline the computational complexity in which we can verify the conditions of Corollary 9.

Remark 10. *We can verify the two conditions in Corollary 9 in $O((m(n+p))^2)$, where n is the number of state variables, p is the number of unknown inputs, and m is the number of modes (Section 3.3, [16]). We notice that the number of variables required to be measured is always less than or equal to $n+p$. ◊*

With the graph-theoretic conditions for structural state and input observability enumerated, we introduce Algorithm 1. Briefly, the algorithm finds the minimum set of state and input variables to ensure that the conditions of Corollary 9 are satisfied. First, the algorithm finds the maximum collection of variables that satisfy the condition of Corollary 9 by constructing the MWMM of $\mathcal{B}([\bar{A}'_1; \dots; \bar{A}'_m; \bar{T}])$, where \bar{T} has as many rows as target-SCCs, and the non-zero column entries of \bar{T} specify the indices of the augmented states that make up each target-SCC. Furthermore, weights are considered on the edges of the bipartite graph such that all edge weights are zero unless the edges connect to a vertex established by \bar{T} at which the weight is set to one. If there is an edge in the MWMM that has a weight of one, then the index of the column vertex connecting the edge is the same index of the augmented state variable that satisfies both conditions in Corollary 9. The algorithm then proceeds to find the minimum set of variables from the maximum collection that still ensure the conditions of Corollary 9.

Algorithm 1 Dedicated solution to \mathcal{P}_1

- 1: **Input:** A structural switched LTI system with $\mathbb{M} = \{1, \dots, m\}$ modes described by $\{\bar{A}_1, \dots, \bar{A}_m, \bar{F}_1, \dots, \bar{F}_m, \bar{Q}_1, \dots, \bar{Q}_m\}$, where $\bar{A}_k \in \{0, \star\}^{n \times n}$, $\bar{F}_k \in \{0, \star\}^{n \times p}$, $\bar{Q}_k \in \{0, \star\}^{p \times p}$, $\forall k \in \{1, \dots, m\}$
 - 2: **Output:** Output $\bar{C} = \mathbb{I}_n^{\mathcal{J}_x}$ and $\bar{D} = \mathbb{I}_p^{\mathcal{J}_d}$, where $\mathcal{J} = \mathcal{J}_x \cup \mathcal{J}_d$, $\mathcal{J}_d = \{i \in \mathcal{J} : i \leq p\}$, and $\mathcal{J}_x = \{i \in \mathcal{J} : i > p\}$
 - 3: **Set** $\bar{A}'_k = \begin{bmatrix} \bar{Q}_k & \mathbf{0} \\ \bar{F}_k & \bar{A}_k \end{bmatrix}$
 - 4: **Compute** the α target-SCCs of $\mathcal{G}(\bigvee_{k=1}^m \bar{A}'_k) = (\mathcal{X}', \mathcal{E}'_{\mathcal{X}', \mathcal{X}'})$, denoted by $\{\mathcal{S}_1, \dots, \mathcal{S}_\alpha\}$
 - 5: **Build** the bipartite graph $\mathcal{B}([\bar{A}'_1; \dots; \bar{A}'_m; \bar{T}]) = (\mathcal{V}_c, \mathcal{V}_r, \mathcal{E}_{\mathcal{V}_c, \mathcal{V}_r})$, where $\bar{T} \in \{0, \star\}^{(n+p) \times \alpha}$ and $\bar{T}_{i,j} = \star$ if $x'_j \in \mathcal{S}_i$ and $\bar{T}_{i,j} = 0$, otherwise. We denote the rows of matrix \bar{A}'_k by $\{r_1^k, \dots, r_{n+p}^k\}$, and the rows of \bar{T} by $\{t_1, \dots, t_\alpha\}$.
 - 6: **Set** the weight of the edges $e \in \mathcal{E}_{\mathcal{V}_c, \mathcal{V}_r}$ to $\begin{cases} 1, & \text{if } e \in (\{t_1, \dots, t_\alpha\} \times \mathcal{V}_c) \cap \mathcal{E}_{\mathcal{V}_c, \mathcal{V}_r} \\ 0, & \text{otherwise} \end{cases}$.
 - 7: **Find** a MWMM \mathcal{M}' of the bipartite graph computed in Step 5, with edges' costs of Step 6.
 - 8: **Set** the column vertices associated with \bar{T} belonging to \mathcal{M}' , i.e., $\mathcal{J}' = \{i : (t_j, c_i) \in \mathcal{M}', j \in \{1, \dots, \alpha\} \text{ and } c_i \in \mathcal{V}_c\}$ and $\mathcal{T} = \{j : (t_j, c_i) \in \mathcal{M}', j \in \{1, \dots, \alpha\}\}$
 - 9: **Set** $\mathcal{J}'' = \{1, \dots, n+p\} \setminus \{i \in \{1, \dots, n+p\} : (r_j^k, c_i) \in \mathcal{M}', k \in \{1, \dots, m\}, j \in \{1, \dots, n+p\}\}$
 - 10: **Set** \mathcal{J}''' to contain one and only one index of a state variable from each target-SCC in $\{\mathcal{S}_s : s \in \{t_1, \dots, t_\alpha\} \setminus \mathcal{T}\}$
 - 11: **Set** $\mathcal{J} = \mathcal{J}' \cup \mathcal{J}'' \cup \mathcal{J}'''$
 - 12: **Set** $\mathcal{J}_d = \{i \in \mathcal{J} : i \leq p\}$, and $\mathcal{J}_x = \{i \in \mathcal{J} : i > p\}$
-

In the next result, we show that Algorithm 1 finds the minimum set of states and inputs to ensure structural state and input observability.

Theorem 11. *Algorithm 1 is sound, i.e., it provides a solution to \mathcal{P}_1 , and the computational complexity of Algorithm 1 is $O((m(n+p) + \alpha)^\varsigma)$, where $\varsigma < 2.373$ is the exponent of the best known computational complexity of performing the product of two square matrices [1].* \circ

Remark 12. *The computational complexity presented in Theorem 11 might not be amenable for ensuring the sensor placement for very large systems. Nonetheless, there are some particular classes of systems for which algorithms with lower computational complexity can be devised. In the next section, we present these classes of systems.* \diamond

Example 1

Let us consider the following linear continuous-time system with two modes $\{\bar{A}_k, \bar{F}_k, \bar{Q}_k\}_{k=1}^2$, where $\bar{A}_k \in \{0, 1\}^{5 \times 5}$, $\bar{F}_k \in \{0, 1\}^{5 \times 1}$, $\bar{Q}_k \in \{0, 1\}$. In particular, $[\bar{A}_1]_{3,1} = 1$, $[\bar{A}_1]_{2,2} = 1$, $[\bar{A}_1]_{4,3} = 1$, $[\bar{A}_2]_{3,2} = 1$, $[\bar{A}_2]_{5,3} = 1$, $[\bar{F}_1]_{2,1} = 1$, $[\bar{F}_2]_{2,1} = 1$, and $\bar{Q}_k = 0, \forall k \in \{1, 2\}$.

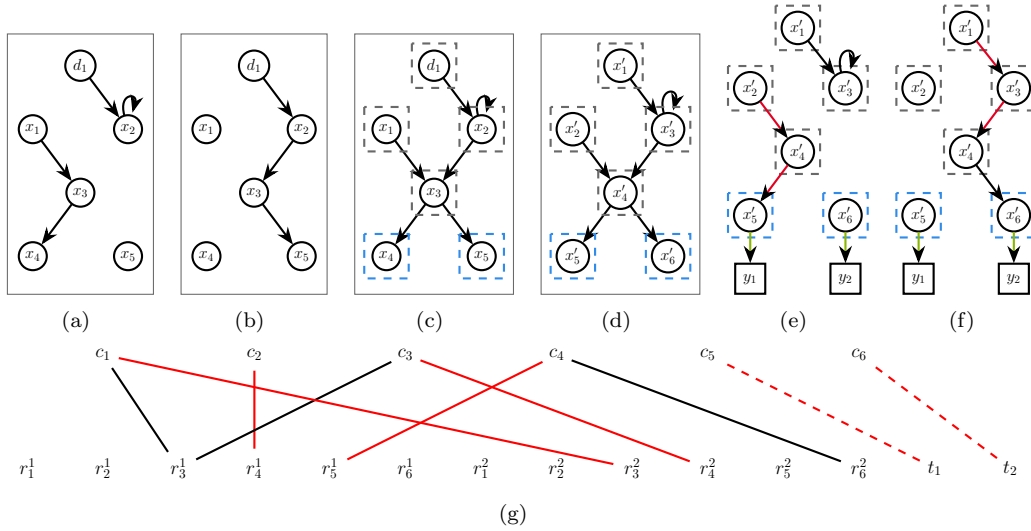


Figure 1: (a) shows A'_1 , (b) shows A'_2 (c) shows the union of the two modes of the continuous-time system with unknown inputs. (d) shows the augmented continuous-time system. Finally, (e) and (f) show the SCCs in dotted black rectangles, the target-SCC in a dotted blue rectangle, and the minimal output sensors and their placement for modes 1 and 2 respectively. (g) shows the bipartite graph $\mathcal{B}([\bar{A}'_1; \bar{A}'_2; \bar{T}])$ with unitary weight on the dotted edge and zero weight on the solid edges. The collection of red edges is the minimum weight maximum matching.

The individual modes of the system are shown in Figure 1 (a)-(b). We apply Algorithm 1 to this system to find the minimum set of dedicated sensors to achieve structural observability. We start by finding the union of the modes. $\bigvee_{k=1}^m \bar{A}'_k$ is given as follows

$$\bar{A}'_1 \vee \bar{A}'_2 = \begin{bmatrix} 0 & 0 & 0 & 0 & 0 & 0 \\ 0 & 0 & 0 & 0 & 0 & 0 \\ 1 & 0 & 1 & 0 & 0 & 0 \\ 0 & 1 & 1 & 0 & 0 & 0 \\ 0 & 0 & 0 & 1 & 0 & 0 \\ 0 & 0 & 0 & 1 & 0 & 0 \end{bmatrix}$$

and is shown in Figure 1 (c) and (d), where (c) shows the union of the modes before the system has been augmented and (d) shows the union of the modes after the system has been augmented and relabeled with state $x' = [d^\top x^\top]^\top$. With the system properly combined and augmented, we continue by finding the target-SCCs of $\mathcal{G}(\bigvee_{k=1}^m \bar{A}'_k)$. We find that there are 6 SCCs, which are outlined in dashed rectangle boxes in Figures 1 (c) and (d). There are 2 target-SCCs, which are outlined in a dashed blue box in Figure 1 (c) and (d), so $\alpha = 2$.

Next, we construct the bipartite graph $\mathcal{B}([\bar{A}'_1; \bar{A}'_2; \bar{T}])$. Since there are two target-SCCs each composed of one state (x'_5, x'_6) , then \bar{T} is as $\bar{T} = \begin{bmatrix} 0 & 0 & 0 & 0 & 0 & 1 \\ 0 & 0 & 0 & 0 & 1 & 0 \end{bmatrix}$. In the bipartite graph, depicted in Figure 1 (g), there are two edges that each connect to one of the two target-SCCs and thus have unitary weight (shown as a dotted line) while the rest of the edges have zero weight (shown as solid lines). In step 7, we find the MWMM \mathcal{M}' , which is shown by the collection of red edges in Figure 1 (g). From the MWMM, we see that there are two edges in the MWMM that are connected to a target-SCC, so $\mathcal{J}' = \{5, 6\}$. In step 9, we find \mathcal{J}'' , which is the set of indices associated with the column vertices of $\bar{A}'_k, \forall k$ that are not in the MWMM (i.e., all of the indices $i = \{1, \dots, n + p\}$ such that c_i are not connected to a red edge in Figure 1 (g)). We notice that there are several different possible minimum weight maximum matchings. One of these possibilities is shown in Figure 1 (g) where, we see that there are no unmatched vertices, so $\mathcal{J}'' = \emptyset$.

In step 10, we find the index of one state variable connected to each target-SCC in which that target-SCC has not already been accounted for in \mathcal{T} . Hence, $\mathcal{J}''' = \emptyset$.

Finally, we can combine $\mathcal{J}' \cup \mathcal{J}'' \cup \mathcal{J}''' = \mathcal{J}$ to obtain the minimum set of indices required to place the sensors for achieving a structurally observable system. We find that $\mathcal{J} = \{5, 6\}$, and the sensor placement is shown in Figure 1 (e) and (f). Since $p = 1$, we note that $\mathcal{J}_x = \{5, 6\}$ and $\mathcal{J}_d = \emptyset$. Therefore, we have $\bar{C} = \mathbb{I}_n^{\mathcal{J}_x}$ and $\bar{D} = \mathbb{I}_p^{\mathcal{J}_d}$ as the solution to \mathcal{P}_1 .

We note that there may be circumstances in which it may not be possible to measure the unknown inputs. Therefore, to reduce the number of unknown inputs that need to be measured, it is necessary to avoid the situation where unknown inputs become left unmatched vertices. Hence, we can include a step in the algorithm to place higher weights on the edges in the bipartite graph that connect two vertices without an unknown input as the left vertex as noted in Remark 13.

Remark 13. *By placing higher weights on the edges in the bipartite graph that do not contain unknown inputs as left vertices, we can ensure that the algorithm avoids measuring unknown inputs where possible.* ◇

4 Special Classes of Systems with Linear-time Computational Complexity

In this section, we will outline two classes of switched LTI systems for which a lower computational complexity can be achieved for the minimum sensor placement problem and provide algorithms and examples for these systems. We start by describing two classes of switched LTI systems that allow for a linear-time computational complexity with respect to the edges. The two classes of switched LTI systems are as follows:

1. switched LTI systems with unknown inputs that do not have memory and remain constant over time, and the system has nodal dynamics in the states;
2. switched LTI systems with nodal dynamics in both inputs and states.

4.1 Switched LTI Systems with memoryless unknown inputs that remain constant over time, and state nodal dynamics

First, we present an example in which the system has nodal dynamics (i.e., self-loops) in the states, and the unknown inputs do not have memory and remain constant over time. We provide the solution obtained from Algorithm 1 for this example. Next, we define an algorithm for this class of systems outlined in Algorithm 2.

Algorithm 2 Dedicated solution for System Class 1

- 1: **input:** A structural switched LTI system with $\mathbb{M} = \{1, \dots, m\}$ modes described by $\{\bar{A}_1, \dots, \bar{A}_m, \bar{F}_1, \dots, \bar{F}_m, \bar{Q}_1, \dots, \bar{Q}_m\}$, where $\bar{A}_k \in \{0, \star\}^{n \times n}$, $\bar{F}_k \in \{0, \star\}^{n \times p}$, $\bar{Q}_k \in \{0\}^{p \times p}$, $\forall k \in \{1, \dots, m\}$, and $d(t) = c, \forall t$
 - 2: **output:** Output $\bar{C} = \mathbb{I}_n^{\mathcal{J}_x}$ and $\bar{D} = \mathbb{I}_p^{\mathcal{J}_d}$, where $\mathcal{J} = \mathcal{J}_x \cup \mathcal{J}_d$, $\mathcal{J}_d = \{i \in \mathcal{J} : i \leq p\}$, and $\mathcal{J}_x = \{i \in \mathcal{J} : i > p\}$
 - 3: **set** $\bar{A}'_k = \begin{bmatrix} \mathbf{0} & \mathbf{0} \\ \bar{F}_k & \bar{A}_k \end{bmatrix}$
 - 4: **find** the α target-SCCs of $\mathcal{G}(\bigvee_{k=1}^m \bar{A}'_k) = (\mathcal{X}', \mathcal{E}'_{\mathcal{X}', \mathcal{X}'})$, denoted by $\{\mathcal{S}_1, \dots, \mathcal{S}_\alpha\}$
 - 5: **Construct** the digraph $\mathcal{G} \equiv \mathcal{G}(\bigvee_{k=1}^m \bar{A}'_k)$
 - 6: **Extend** \mathcal{G} adding the following nodes:
 - ▷ a virtual source node s ;
 - ▷ a virtual target node t ;
 - ▷ an ancillary node for each target-SCC denoted by a_1, \dots, a_α .
 In addition, add the following edges:
 - ▷ an edge from node s to each unknown input;
 - ▷ an edge from each node in the \mathcal{S}_i to a_i , for $i = 1, \dots, \alpha$;
 - ▷ an edge from a_i to t , for $i = 1, \dots, \alpha$;
 - ▷ an edge from each unknown input to t .
 - 7: **set** the edge capacities to

$$\begin{cases} 1, & \text{if the edge connects the unknown inputs} \\ & \text{to the virtual target node} \\ 2, & \text{otherwise} \end{cases}$$
 - 8: **find** the vertex-disjoint paths denoted by $\{\mathcal{T}_1, \dots, \mathcal{T}_z\}$ of the digraph constructed in the previous steps starting in the virtual source node s and ending in the virtual target node t using the Ford Fulkerson algorithm to find the maximum flow
 - 9: **Set** \mathcal{J}' to contain the indices of each node that is connected to the ancillary variables a_1, \dots, a_α in a disjoint path and the indices of unknown input nodes if they connect to the target node in a disjoint path
 - 10: **Set** \mathcal{J}'' to contain a single index of a state variable from each target-SCC not accounted for in \mathcal{J}'
 - 11: **Set** $\mathcal{J} = \mathcal{J}' \cup \mathcal{J}''$
 - 12: **Set** $\mathcal{J}_d = \{i \in \mathcal{J} : i \leq p\}$, and $\mathcal{J}_x = \{i \in \mathcal{J} : i > p\}$
-

Next, we prove the soundness and derive the computational complexity of Algorithm 2.

Theorem 14. *Algorithm 2 is sound, i.e., it provides a solution to \mathcal{P}_1 for systems in which the unknown inputs do not have memory and remain constant over time, and the system has nodal dynamics in the states. The computational complexity of Algorithm 2 is $O((n+p)^2)$, where n is the number of states $x(t) \in \mathbb{R}^n$ and p is the number of unknown inputs $d(t) \in \mathbb{R}^p$. \circ*

We give a brief overview of how the algorithm presented in Algorithm 2 differs from Algorithm 1. The main difference is in Algorithm 1 where we must find a MWMM of the bipartite graph $\mathcal{B}([\bar{A}'_1; \dots; \bar{A}'_m; \bar{T}])$ whereas in Algorithm 2, we only need to find the vertex-disjoint paths, which is why we can reduce the computational complexity.

In the next example, we illustrate the results after applying both Algorithm 1 and Algorithm 2.

Example 2

Let us consider the following linear continuous-time system with three modes $\{\bar{A}_k, \bar{F}_k, \bar{Q}_k\}_{k=1}^3$, where $\bar{A}_k \in \{0, 1\}^{4 \times 4}$, $\bar{F}_k \in \{0, 1\}^{4 \times 1}$, $\bar{Q}_k \in \{0, 1\}$. In particular,

$$A_1 = \begin{bmatrix} 1 & 0 & 0 & 0 \\ 0 & 0 & 0 & 0 \\ 1 & 0 & 1 & 0 \\ 0 & 0 & 0 & 0 \end{bmatrix}, A_2 = \begin{bmatrix} 0 & 0 & 0 & 0 \\ 0 & 1 & 0 & 0 \\ 0 & 1 & 1 & 0 \\ 0 & 0 & 0 & 0 \end{bmatrix}, A_3 = \begin{bmatrix} 1 & 0 & 0 & 0 \\ 0 & 1 & 0 & 0 \\ 0 & 0 & 1 & 0 \\ 0 & 0 & 1 & 1 \end{bmatrix},$$

$$[\bar{F}_1]_{1,1} = 1, [\bar{F}_2]_{2,1} = 1, [\bar{F}_3]_{1,1} = 1, [\bar{F}_3]_{2,1} = 1, \text{ and } \bar{Q}_k = 0, \forall k \in \{1, 2, 3\}.$$

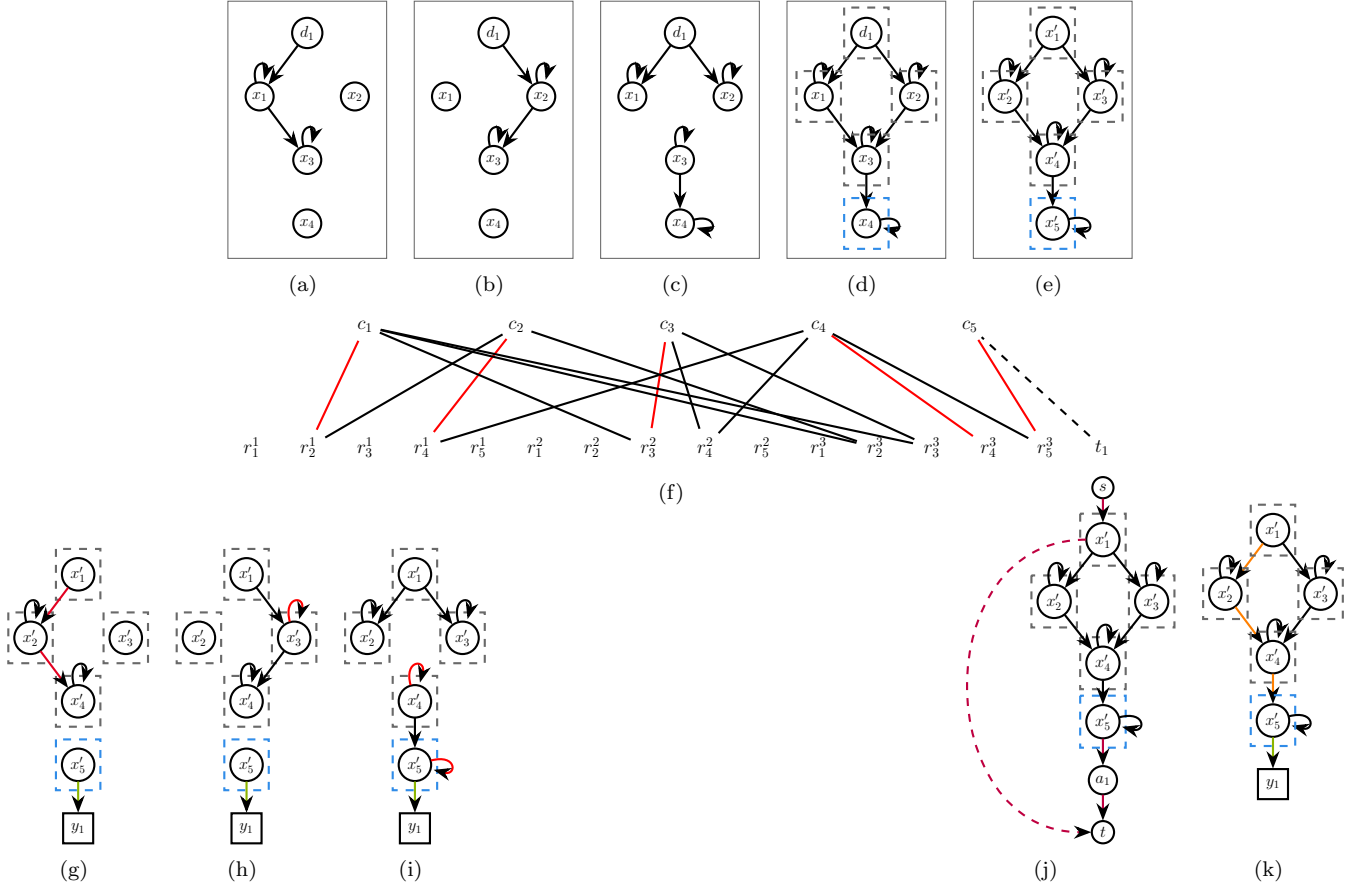


Figure 2: (a) shows A'_1 , (b) shows A'_2 (c) shows A'_3 and (d) shows the union of the three modes of the continuous-time system with unknown inputs (e) shows the augmented continuous-time system. (f) shows the bipartite graph $\mathcal{B}([\bar{A}'_1; \bar{A}'_2; \bar{A}'_3; \bar{T}])$ with unitary weight on the dotted edge and zero weight on the solid edges. The collection of red edges is the minimum weight maximum matching. (g)-(i) show the SCCs in dotted black rectangles, the target-SCC in a dotted blue rectangle, and the minimal output sensors and their placement for all three modes after applying Algorithm 1 (j) shows the digraph with the extra nodes and edges (shown in purple) added in steps 6 and 7. The dashed purple line signifies that the edge has a weight of 2. (k) shows the vertex disjoint path in orange and the solution for the minimal output sensors placement after applying Algorithm 2.

The individual modes of the system are shown in Figure 2 (a)-(c). We apply Algorithm 1 to this system to find the minimum set of dedicated sensors to achieve structural observability. We start by finding the union of the modes. $\bigvee_{k=1}^m \bar{A}'_k$ is given as follows

$$\bar{A}'_1 \vee \bar{A}'_2 \vee \bar{A}'_3 = \begin{bmatrix} 0 & 0 & 0 & 0 & 0 \\ 1 & 1 & 0 & 0 & 0 \\ 1 & 0 & 1 & 0 & 0 \\ 0 & 1 & 1 & 1 & 0 \\ 0 & 0 & 0 & 1 & 1 \end{bmatrix}$$

and is shown in Figure 2 (d) and (e), where (d) shows the union of the modes before the system has been augmented and (e) shows the union of the modes after the system has been augmented and relabeled with state $x' = [d^\top x^\top]^\top$. With the system properly combined and augmented, we continue by finding the target-SCCs of $\mathcal{G}(\bigvee_{k=1}^m \bar{A}'_k)$. We find that there are 5 SCCs, which are outlined in dashed rectangle boxes in Figure 2 (d)-(e). We also find that there is 1 target-SCC, which is outlined in a dashed blue box in Figure 2 (d)-(e), so $\alpha = 1$.

We construct the bipartite graph $\mathcal{B}([\bar{A}'_1; \bar{A}'_2; \bar{A}'_3; \bar{T}])$. First, we note that since there is only one target-SCC composed of one state (x'_5), then $\bar{T} = [0 \ 0 \ 0 \ 0 \ 1]$. In the bipartite graph depicted in Figure 2 (f), there is one edge that connects to the target-SCC and thus has unitary weight (shown as a dotted line) while the rest of the edges have zero weight (shown as solid lines). In step 7, we find the MWMM \mathcal{M}' . There are different possible MWMM, one of which is shown by the collection of red edges in Figures 2 (f). From the MWMM, we see that there aren't any edges in the MWMM that are connected to the target-SCC, so $\mathcal{J}' = \emptyset$. In step 9, for the MWMM in Figure 2 (f), we find $\mathcal{J}'' = \emptyset$,

which is the set of indices associated with the column vertices of $\bar{A}'_k, \forall k$ that are not in the MWMM (i.e., all of the indices $j = \{1, \dots, n + p\}$ such that c_j are not connected to a red edge in Figure 2 (f)).

In step 10, we find the index of one state variable connected to each target-SCC for each not already accounted target-SCC. Hence, $\mathcal{J}''' = \{5\}$.

Finally, we can combine $\mathcal{J}' \cup \mathcal{J}'' \cup \mathcal{J}''' = \mathcal{J} = \{5\}$ to obtain the minimum set of indices required to place the sensors for achieving a structurally observable system. Since $p = 1$, we find that $\mathcal{J}_x = \{5\}$ and $\mathcal{J}_d = \emptyset$. Therefore, we have $\bar{C} = \mathbb{I}_n^{\mathcal{J}_x}$ and $\bar{D} = \mathbb{I}_p^{\mathcal{J}_d}$.

Next, we apply Algorithm 2 to this system. We again start by finding the target-SCCs of $\mathcal{G}(\bigvee_{k=1}^m \bar{A}'_k)$, which are outlined in blue dashed boxes in Figure 2 (d)-(e). Then, we construct the system digraph $\mathcal{G}(\bigvee_{k=1}^m \bar{A}'_k)$ along with the additional virtual nodes, ancillary nodes, edges, and appropriate edge capacities described in step 7, which is shown in Figure 2 (j). Next, we find the vertex-disjoint paths of the digraph pictured in Figure 2 (j), which are shown as orange paths in Figures 2 (k). We find one vertex disjoint path with ending in node 5, so $\mathcal{J}' = \{5\}$ (see Figure 2 (k)). Since there is only one target-SCC, which has already been accounted for in \mathcal{J}' , then we find that $\mathcal{J}'' = \emptyset$. Combining both sets, we find the same solution as calculated in Algorithm 1, namely $\mathcal{J} = \mathcal{J}' \cup \mathcal{J}'' = \{5\}$. Finally, this results in the same \mathcal{J}_d and \mathcal{J}_x sets as well.

Remark 15. In [14], the authors present a quadratic (in the number of vertices) time-complexity algorithm to compute a set of independent paths in a digraph between pairs of given vertices. The computational complexity for finding the induced disjoint paths problem can be reduced to linear-time (in the number of vertices) if the graph is planar as seen in [13]. A digraph is planar if it can be drawn in the plane without any edge intersections. As such, finding the minimum sensors in Examples 2 and 3 can be reduced to a linear-time computational complexity with respect to the number of vertices plus edges. \diamond

4.2 Systems with Nodal Dynamics

For digraphs that are spanned by cycles, finding the minimum sensor placement only requires finding the target-SCCs [19]. Next, we present an example where the digraph is not only spanned by cycles but has nodal dynamics meaning every state has a self-loop. We will show through this example that the conditions for finding the minimum number of dedicated sensors to ensure structural state and input observability for digraphs spanned by cycles boils down to finding the target-SCCs. We present Algorithm 3, which finds the dedicated solution for the System Class 2 (i.e., nodal dynamics).

Algorithm 3 Dedicated solution for System Class 2

- 1: **input:** A structural switched LTI system with $\mathbb{M} = \{1, \dots, m\}$ modes described by $\{\bar{A}_1, \dots, \bar{A}_m, \bar{F}_1, \dots, \bar{F}_m, \bar{Q}_1, \dots, \bar{Q}_m\}$, where $\bar{A}_k \in \{0, \star\}^{n \times n}$, $\bar{F}_k \in \{0, \star\}^{n \times p}$, $\bar{Q}_k \in \{0, \star\}^{p \times p}$, and the diagonal entries of A_k and Q_k are nonzero for all $k \in \{1, \dots, m\}$
 - 2: **output:** Output $\bar{C} = \mathbb{I}_n^{\mathcal{J}_x}$ and $\bar{D} = \mathbb{I}_p^{\mathcal{J}_d}$, where $\mathcal{J} = \mathcal{J}_x \cup \mathcal{J}_d$, $\mathcal{J}_d = \{i \in \mathcal{J} : i \leq p\}$, and $\mathcal{J}_x = \{i \in \mathcal{J} : i > p\}$
 - 3: **set** $\bar{A}'_k = \begin{bmatrix} \bar{Q}_k & \mathbf{0} \\ \bar{F}_k & \bar{A}_k \end{bmatrix}$
 - 4: **find** the α target-SCCs of $\mathcal{G}(\bigvee_{k=1}^m \bar{A}'_k) = (\mathcal{X}', \mathcal{E}_{\mathcal{X}', \mathcal{X}'})$, denoted by $\{\mathcal{S}_1, \dots, \mathcal{S}_\alpha\}$
 - 5: **Set** \mathcal{J} to contain one and only one index of a state variable from each target-SCC in $\{\mathcal{S}_s : s \in \{1, \dots, \alpha\}\}$
 - 6: **Set** $\mathcal{J}_d = \{i \in \mathcal{J} : i \leq p\}$, and $\mathcal{J}_x = \{i \in \mathcal{J} : i > p\}$
-

Theorem 16. Algorithm 3 is sound, i.e., it provides a solution to \mathcal{P}_1 for systems with nodal dynamics. The computational complexity of Algorithm 3 is $O((n + p)^2)$, where n is the number of states $x(t) \in \mathbb{R}^n$, and p is the number of unknown inputs. \diamond

We note in Remark 17 that the solution for this example can be found in a distributed fashion.

Remark 17. We remark that a distributed solution can be used to find the minimum solution for nodal systems (i.e., a system with self-loops) [21]. \diamond

We give a brief overview of how the algorithm presented in Algorithm 3 differs from Algorithm 1. The main difference is in Algorithm 3 we only need to find the target-SCCs, which is why we can reduce the computational complexity.

In the next example, we illustrate the results after applying both Algorithm 1 and Algorithm 3 to a system with nodal dynamics.

Let us consider the following linear continuous-time system with two modes $\{\bar{A}_k, \bar{F}_k, \bar{Q}_k\}_{k=1}^2$, where $\bar{A}_k \in \{0, 1\}^{2 \times 2}$, $\bar{F}_k \in \{0, 1\}^{2 \times 1}$, $\bar{Q}_k \in \{0, 1\}$. In particular, $[\bar{A}_1]_{1,1} = 1$, $[\bar{A}_2]_{2,2} = 1$, $[\bar{F}_1]_{1,1} = 1$, $[\bar{F}_2]_{2,1} = 1$, and $\bar{Q}_k = 1, \forall i \in \{1, 2\}$.

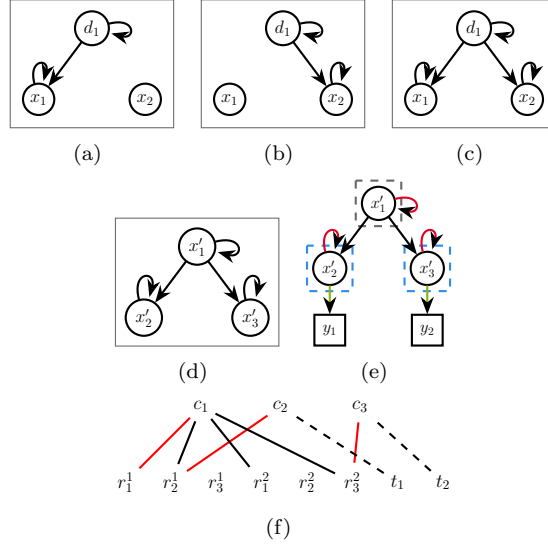


Figure 3: (a) shows A'_1 (b) shows A'_2 (c) shows the union of the two modes of the continuous-time system with unknown inputs, and (d) shows the augmented continuous-time system. (e) shows the SCCs in dotted black rectangles, the target-SCCs in a dotted blue rectangle, and the minimal output sensors and their placement. (f) shows the bipartite graph $\mathcal{B}([\bar{A}'_1; \bar{A}'_2; \bar{T}])$ with unitary weight on the dotted edge and zero weight on the solid edges. The collection of red edges is the minimum weight maximum matching.

The individual modes of the system are shown in Figure 3 (a)-(b). We apply Algorithm 1 to this system to find the minimum set of dedicated sensors to achieve structural observability. We start by finding the union of the modes.

$\bigvee_{k=1}^m \bar{A}'_k$ is given as $\bar{A}'_1 \vee \bar{A}'_2 = \begin{bmatrix} 1 & 0 & 0 \\ 1 & 1 & 0 \\ 1 & 0 & 1 \end{bmatrix}$ and is shown in Figure 3 (c) and (d), where (c) shows the union of the modes before the system has been augmented and (d) shows the union of the modes after the system has been augmented and relabeled with state $x' = [d^T \ x^T]^T$. With the system properly combined and augmented, we continue by finding the target-SCCs of $\mathcal{G}(\bigvee_{k=1}^m \bar{A}'_k)$. We find that there are 3 SCCs, which are outlined in dashed rectangle boxes in Figure 3 (e). We also find that there are 2 target-SCCs, which are outlined in a dashed blue box in Figure 3 (e), so $\alpha = 2$.

We construct the bipartite graph $\mathcal{B}([\bar{A}'_1; \bar{A}'_2; \bar{T}])$. Since there are two target-SCCs each composed of one state (x'_2, x'_3), then \bar{T} is as $\bar{T} = \begin{bmatrix} 0 & 0 & 1 \\ 0 & 1 & 0 \end{bmatrix}$. In the bipartite graph depicted in Figure 3 (f), there are two edges that each connect to one of the two target-SCCs and thus have unitary weight (shown as a dotted line) while the rest of the edges have zero weight (shown as solid lines). In step 7, we find the MWMM \mathcal{M}' , which is shown by the collection of red edges in Figure 3 (f). From the MWMM, we see that there aren't any edges in the MWMM that are connected to a target-SCC, so $\mathcal{J}' = \emptyset$. In step 9, we find \mathcal{J}'' , which is the set of indices associated with the column vertices \bar{A}' that are not in the MWMM (i.e., all of the indices $j = \{1, \dots, n + p\}$ such that c_j are not connected to a red edge in Figure 3 (f)). We find that $\mathcal{J}'' = \emptyset$. In step 10, we find the index of one state variable connected to each target-SCC for each not already accounted target-SCC. Hence, $\mathcal{J}''' = \{2, 3\}$.

Finally, we can combine $\mathcal{J}' \cup \mathcal{J}'' \cup \mathcal{J}''' = \mathcal{J} = \{2, 3\}$ to obtain the minimum set of indices required to place the sensors for achieving a structurally observable system. The sensor placement is shown in Figure 3 (e). Since $p = 1$, we note that $\mathcal{J}_x = \{2, 3\}$ and $\mathcal{J}_d = \emptyset$. Therefore, we have $\bar{C} = \mathbb{I}_n^{\mathcal{J}_x}$ and $\bar{D} = \mathbb{I}_p^{\mathcal{J}_d}$.

Next, we apply Algorithm 3 to this system. After augmenting the system, we again start by finding the target-SCCs of $\mathcal{G}(\bigvee_{k=1}^m \bar{A}'_k)$, which are outlined in the dashed blue boxes in Figure 3 (f). Next, we find a single state in each of the two target-SCCs and add their indices to \mathcal{J} . Hence, $\mathcal{J} = \{2, 3\}$, which we note is the same result achieved by Algorithm 1.

5 Real-World Example

In this section, we find the minimum sensor placement for a real-world example from power systems by considering the IEEE 5-bus system [24], which has three generators and two loads. Through linearization, we can model this system as a continuous-time switched LTI system with unknown inputs by considering two modes. One mode is the working system, and the second mode contains a fault that disconnects generator 1 to load 1, which corresponds to the connection between x_{14} and x_{10} being eliminated. The unknown inputs d_1 and d_2 capture the unknown amount of load consumed by loads 1 and 2, respectively. Table 1 describes the states and unknown inputs of the network. The shaded rows in the table correspond to the unknown inputs. The variables/nodes that are not listed in the table but appear in the system digraph correspond to the internal variables that connect the different bus, generators, and loads. The blue nodes correspond to load 1. The orange nodes correspond to load 2. The green nodes correspond to generator 1. The red nodes correspond to generator 2. The gray nodes correspond to generator 3.

| Description | Node |
|--|----------|
| frequency of G_1 | x_1 |
| turbine output mechanical power of G_1 | x_2 |
| steam valve opening position of G_1 | x_3 |
| frequency of G_2 | x_4 |
| turbine output mechanical power of G_2 | x_5 |
| steam valve opening position of G_2 | x_6 |
| frequency of G_3 | x_7 |
| turbine output mechanical power of G_3 | x_8 |
| steam valve opening position of G_3 | x_9 |
| unknown uncertainty L_1 | d_1 |
| load consumed by L_1 | x_{10} |
| unknown uncertainty of L_2 | d_2 |
| load consumed by L_2 | x_{12} |

Table 1: States and Unknown Inputs for IEEE 5-bus system

The union of the two modes are shown in Figure 4. Since the system possesses nodal dynamics on all both the inputs and states, we apply Algorithm 3 to this system to find the minimum set of dedicated sensors to achieve structural observability. We start by finding the union of the modes, which is shown in Figure 4. Next, we augmented the system and relabeled it with state $x' = [d^\top x^\top]^\top$. With the system properly combined and augmented, we continue by finding the target-SCCs of $\mathcal{G}(\bigvee k = 1^m \bar{A}'_k)$. We find that there are 3 SCCs, which are outlined in dashed polygons in Figure 4. We also find that there is 1 target-SCCs, which is outlined in a dashed blue polygon in Figure 4, so $\alpha = 1$. Next, we find a single state in the target-SCCs and add its indices to \mathcal{J} . In this real-world example, it makes most sense to measure the load consumed from either load. Hence, $\mathcal{J} = \{12\}$ or $\mathcal{J} = \{10\}$.

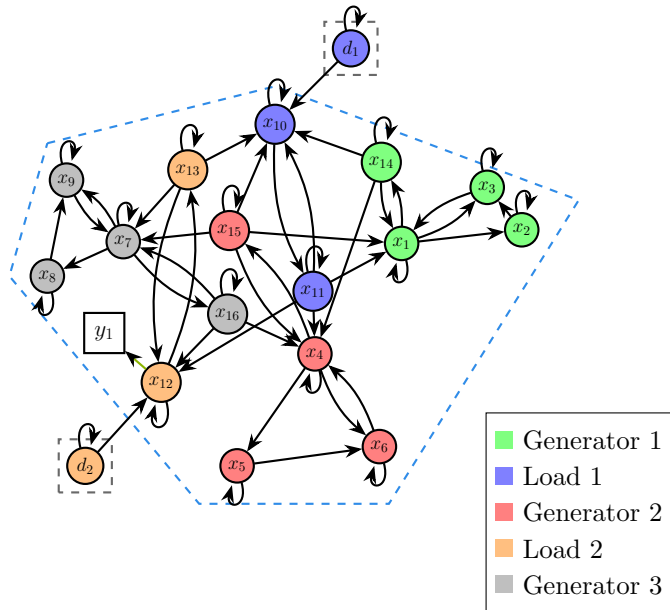


Figure 4: This figure shows the union of the two modes of the continuous-time system with unknowns for the IEEE 5-bus system. The SCCs are outlined by two dotted black rectangles, and the target-SCCs is outlined by a dotted blue polygon. The minimum output sensor and its placement is shown by y_1 .

6 Conclusions

In this paper, we investigated the structural state and input observability of continuous-time switched LTI systems under unknown inputs when unknown inputs can be modeled as LTI systems. To this end, we derived necessary and sufficient conditions for the structural state and input observability of continuous-time switched LTI systems. These conditions can be verified in polynomial-time, more precisely in $O((m(n+p))^2)$, where n is the number of state variables, p is the number of unknown inputs, and m is the number of modes. Additionally, accounting for feed-forward scenarios, we addressed the minimum sensor placement for these systems designing an algorithm with a computational complexity of $O((m(n+p) + \alpha)^{2.373})$, where α is the number of target strongly connected components.

Finally, we examined various assumptions on both the system and unknown inputs (latent space) dynamics. These assumptions translated into imposing additional structure on the problem, which allowed for finding solutions in a more efficient manner (i.e., with lower computational complexity). These algorithms are suitable to handle large-scale systems.

Appendix

Proof of Theorem 7: The continuous-time switched LTI system with unknown inputs described in (1a), (1b), and (1c') may be re-written as the following augmented continuous-time switched LTI system where the new augmented system is $x' = [d^T \ x^T]^T$,

$$\dot{x}'(t) = \underbrace{\begin{bmatrix} Q_{\sigma(t)} & \mathbf{0} \\ F_{\sigma(t)} & A_{\sigma(t)} \end{bmatrix}}_{A'_{\sigma(t)}} x'(t) \text{ and } y'(t) = \underbrace{[D \ C]}_{C'_{\sigma(t)}} x'(t). \quad (2)$$

Moreover, let $\mathbb{M} = \{1, \dots, m\}$ be the ordered finite set of modes where the function $\sigma(t)$ is constant. Then, we have that $A'_k = \begin{bmatrix} Q_k & \mathbf{0} \\ F_k & A_k \end{bmatrix}$ and $C' = [D \ C]$. Therefore, when the system in (1a), (1b), and (1c') is structurally state and input observable, it is equivalent to when the system in (2) is structurally state observable. Interestingly, despite the fact that observability and controllability are not dual in general for switched LTI systems, in Theorem 4 in [17], the authors showed that switched LTI systems are dual in the case of circulatory switching (see Definition 3 in [17]). From Remark 3 in [16], it readily follows that, in the context of structural switched LTI systems, the order of the switches does not play a role in attaining structural controllability. Therefore, in particular, it follows that structural controllability can be attained in the case of circulatory switching. As such, we can leverage Theorem 4 in [17] and invoke duality between structural controllability and structural

(state) observability. Hence, by Theorem 3 of [20], the system in (2) is structurally observable whenever the conditions (i) and (ii) hold.

Proof of Corollary 9: First, we construct the augmented system (2) from the original system (1). Second, we need to ensure that the conditions in Theorem 7 are satisfied. When the digraph $\mathcal{G}(\bigvee_{k=1}^m \bar{A}'_k, \bar{C}')$ has no non-accessible output vertices, it is equivalent to the existence of an edge from a state variable in each target-SCC $\mathcal{G}(\bigvee_{k=1}^m \bar{A}'_k)$ to an output vertex of $\mathcal{G}(\bigvee_{k=1}^m \bar{A}'_k, \bar{C}')$. Thus, condition (i) is equivalent to condition (i) of Theorem 7. Subsequently, we recall the result from [6], which states that for $\bar{M} \in \{0, \star\}^{n_1 \times n_2}$, when the $\text{g-rank}(\bar{M}) = \min\{n_1, n_2\}$, it is equivalent to when there exists a maximum matching of $\mathcal{B}(\bar{M})$ of size $\min\{n_1, n_2\}$. Hence, by the previous result, condition (ii) is equivalent to condition (ii) of Theorem 7.

Proof of Theorem 11: To address the problem \mathcal{P}_1 , we augment the system in (1a) and (1b) to be written as in (2) where $x' = [d^\top \ x^\top]$. With this augmented system, Algorithm 1 constructs three minimum sets of dedicated outputs that combine to satisfy the two conditions outlined in Theorem 7, which guarantee structural state and input observability. Minimality of the combined sets is ensured as we use maximum matchings to build the three sets.

Subsequently, we use Algorithm 1 with the structural switched LTI system with $\mathbb{M} = \{1, \dots, m\}$ modes described by the matrices $\{\bar{A}'_1, \dots, \bar{A}'_m\}$, where the matrices \bar{A}'_k are defined as $\bar{A}'_k = \begin{bmatrix} \bar{Q}_k & \mathbf{0} \\ \bar{F}_k & \bar{A}_k \end{bmatrix}, \forall k \in \mathbb{M}$.

First, we observe that \mathcal{J}' comprises a minimum set of dedicated outputs, which maximizes the $\text{g-rank}([\bar{A}'_1; \dots; \bar{A}'_m; \mathbb{I}_{(n+p)}^{\mathcal{J}'})$, where $\mathbb{I}_{(n+p)}^{\mathcal{J}'}$ is a diagonal matrix whose entries in \mathcal{J}' are nonzero. Concatenating $[\bar{A}'_1; \dots; \bar{A}'_m]$ with $\mathbb{I}_{(n+p)}^{\mathcal{J}'}$ increases the generic rank by $|\mathcal{J}'|$ and produces dedicated outputs assigned to state variables in distinct target-SCCs. In fact, $\mathcal{B}([\bar{A}'_1; \dots; \bar{A}'_m])$ yields a MWMM \mathcal{M} with weight 0 and size $|\mathcal{M}|$. Hence, by the result from [6] used in the proof of Corollary 9, it follows that $\text{g-rank}([\bar{A}'_1; \dots; \bar{A}'_m; \mathbb{I}_{(n+p)}^{\mathcal{J}'}) = |\mathcal{M}|$.

Next, a MWMM \mathcal{M}' of $\mathcal{B}([\bar{A}'_1; \dots; \bar{A}'_m; \bar{T}^\top])$ has size $|\mathcal{M}'|$. This corresponds to an increase in $\text{g-rank}([\bar{A}'_1; \dots; \bar{A}'_m; \mathbb{I}_{(n+p)}^{\mathcal{J}' \cup \mathcal{J}''}])$ from $\text{g-rank}([\bar{A}'_1; \dots; \bar{A}'_m; \mathbb{I}_{(n+p)}^{\mathcal{J}'})$ of $|\mathcal{M}'| - |\mathcal{M}|$. Observe that, by the construction of the matrix \bar{T} , we have that $\mathbb{I}_{(n+p)}^{\mathcal{J}''}$ corresponds to dedicated outputs assigned to state variables in distinct target-SCCs. This means that $|\mathcal{J}''|$ target-SCCs will have outgoing edges to different outputs of the system digraph. This is necessary to satisfy condition (i) of Theorem 7 but may not be sufficient.

Therefore, we have to finally consider a third set, \mathcal{J}''' , to ensure that condition (i) is fulfilled. In other words, there might still be target-SCCs that are not accounted for by state variables indexed in $\mathcal{J}' \cup \mathcal{J}''$, which we account for in \mathcal{J}''' .

By minimizing the number of additional dedicated outputs $\mathbb{I}_{(n+p)}^{\mathcal{J}'''}$, in step 8, we satisfy condition (ii) in Theorem 7 since $\text{g-rank}([\bar{A}'_1; \dots; \bar{A}'_m; \mathbb{I}_{(n+p)}^{\mathcal{J}' \cup \mathcal{J}'' \cup \mathcal{J}'''}]) = n + p$. Additionally, the set \mathcal{J}''' of minimum extra dedicated outputs, found in step 9, ensures that there are not state vertices that do not access at least one output vertex in $\mathcal{G}(\bigvee_{k=1}^m \bar{A}'_k, \mathbb{I}_{(n+p)}^{\mathcal{J}})$, where $\mathcal{J} = \mathcal{J}' \cup \mathcal{J}'' \cup \mathcal{J}'''$, thereby fulfilling condition (i) of Theorem 7. Notice that $\mathbb{I}_{(n+p)}^{\mathcal{J}'''}$ are not assigned to previously assigned target-SCCs, as they would have been considered in $\mathbb{I}_{(n+p)}^{\mathcal{J}'}$.

Consequently, by the construction, setting $\mathcal{J} = \mathcal{J}' \cup \mathcal{J}'' \cup \mathcal{J}'''$ in step 10 yields a solution $\mathbb{I}_{(n+p)}^{\mathcal{J}}$ that is minimal, ensuring both conditions of Corollary 9. Notice that the produced solution easily translates to the original problem \mathcal{P}_1 solution by setting the originals $\bar{C} = \mathbb{I}_n^{\mathcal{J}_x}$ and $\bar{D} = \mathbb{I}_p^{\mathcal{J}_d}$, where $\mathcal{J}_x = \{i \in \mathcal{J} : i > p\}$ and $\mathcal{J}_d = \{i \in \mathcal{J} : i \leq p\}$.

The computational complexity of Algorithm 1 comes from the step with the highest computational cost (step 6) since the remaining steps of the algorithm have lower complexity. The computational complexity of step 6 can be solved by resorting to the Hungarian algorithm [15] that finds a MWMM of $\mathcal{B}([\bar{A}'_1; \dots; \bar{A}'_m; \bar{T}])$ in $O(\max\{|\mathcal{V}_r|, |\mathcal{V}_c|\}^\varsigma)$, where \mathcal{V}_r and \mathcal{V}_c are defined in step 4 and $\varsigma < 2.373$ is the exponent of the best known computational complexity of performing the product of two square matrices. Since $|\mathcal{V}_c| \leq |\mathcal{V}_r|$, this results in a computational cost of $O(|\mathcal{V}_r|^\varsigma) = O((m(n+p) + \alpha)^\varsigma)$.

Proof of Theorem 14: To prove the soundness of Algorithm 2, we need to verify the two conditions in Corollary 9. In step 9, the set \mathcal{J}' assigns an output to the nodes connected to the virtual target node t that are associated with the obtained disjoint paths that start from the virtual source node and end in virtual target node. Subsequently, in step 10, \mathcal{J}'' assigns an output to a state variable of each target-SCC that is not contemplated in the set \mathcal{J}' . Therefore, $\mathcal{J} = \mathcal{J}' \cup \mathcal{J}''$ ensures condition (i) of Corollary 9. Next, we set $\bar{C}' = \mathbb{I}^{\mathcal{J}}$.

Now, we can see that $\mathcal{B}([\bar{A}'_1; \dots; \bar{A}'_m; \bar{C}'])$ has a maximum matching of size $n + p$, so condition (ii) of Corollary 9 is satisfied, corresponding to a decomposition of the system's digraph into paths and cycles that span the digraph, whose paths end in output vertices. This property holds because the system's digraph $\mathcal{G}(\bigvee_{k=1}^m \bar{A}'_k)$ is spanned by the paths obtained in step 8, together with the edges that connect the end of the paths to the respective outputs and the cycles (self-loops) from the state variables that do not belong to the paths. Thus, Algorithm 2 is sound.

The computational complexity of Algorithm 2 comes from the step with the highest computational cost (step 7). The computational complexity of step 7 can be solved by finding the vertex disjoint paths, which is linear in the number of edges [14], and hence, quadratic in the number of vertices.

Proof of Theorem 16: Since the system is spanned by cycles as a result of the nodal dynamics, then the system is structurally

state and input observable if and only if all of the states and inputs are accessible [23]. Hence, by guaranteeing that at least one state in each target-SCCs is measured, we ensure that the system is accessible.

The complexity follows from the fact that each step is linear in time, except for finding the target-SCCs where the computational complexity is linear in the number of nodes plus edges resulting from Tarjan's strongly connected components algorithm [7], which in the worst case is $O((n + p)^2)$.

References

- [1] Josh Alman and Virginia Vassilevska Williams. A refined laser method and faster matrix multiplication. In *Proceedings of the 2021 ACM-SIAM Symposium on Discrete Algorithms (SODA)*, pages 522–539. SIAM, 2021.
- [2] Rajeev Alur. *Principles of cyber-physical systems*. MIT Press, 2015.
- [3] Taha Boukhobza. Sensor location for discrete mode observability of switching linear systems with unknown inputs. *Automatica*, 48(7):1262–1272, 2012.
- [4] Taha Boukhobza and Frédéric Hamelin. Observability of switching structured linear systems with unknown input. a graph-theoretic approach. *Automatica*, 47(2):395–402, 2011.
- [5] Taha Boukhobza, Frédéric Hamelin, G Kabadi, and Samir Aberkane. Discrete mode observability of switching linear systems with unknown inputs. a graph-theoretic approach. *IFAC Proceedings Volumes*, 44(1):6616–6621, 2011.
- [6] Christian Commault, Jean-Michel Dion, and Jacob W van der Woude. Characterization of generic properties of linear structured systems for efficient computations. *Kybernetika*, 38(5):503–520, 2002.
- [7] Thomas H Cormen, Charles E Leiserson, Ronald L Rivest, and Clifford Stein. *Introduction to algorithms*. MIT press, 2009.
- [8] ML Corradini and A Cristofaro. A sliding-mode scheme for monitoring malicious attacks in cyber-physical systems. *IFAC-PapersOnLine*, 50(1):2702–2707, 2017.
- [9] Dongsheng Du, Bin Jiang, and Peng Shi. *Fault tolerant control for switched linear systems*. Springer, 2015.
- [10] Faezeh Farivar, Mohammad Sayad Haghghi, Alireza Jolfaei, and Mamoun Alazab. Artificial intelligence for detection, estimation, and compensation of malicious attacks in nonlinear cyber-physical systems and industrial iot. *IEEE transactions on industrial informatics*, 16(4):2716–2725, 2019.
- [11] Gaurav Gupta, Sérgio Pequito, and Paul Bogdan. Re-thinking eeg-based non-invasive brain interfaces: Modeling and analysis. In *2018 ACM/IEEE 9th International Conference on Cyber-Physical Systems (ICCP)*, pages 275–286. IEEE, 2018.
- [12] R Matthew Hutchison, Thilo Womelsdorf, Elena A Allen, Peter A Bandettini, Vince D Calhoun, Maurizio Corbetta, Stefania Della Penna, Jeff H Duyn, Gary H Glover, Javier Gonzalez-Castillo, et al. Dynamic functional connectivity: promise, issues, and interpretations. *Neuroimage*, 80:360–378, 2013.
- [13] Ken-ichi Kawarabayashi and Yusuke Kobayashi. A linear time algorithm for the induced disjoint paths problem in planar graphs. *Journal of Computer and System Sciences*, 78(2):670–680, 2012.
- [14] Ken-ichi Kawarabayashi, Yusuke Kobayashi, and Bruce Reed. The disjoint paths problem in quadratic time. *Journal of Combinatorial Theory, Series B*, 102(2):424–435, 2012.
- [15] Harold W Kuhn. The hungarian method for the assignment problem. *Naval research logistics quarterly*, 2(1-2):83–97, 1955.
- [16] Xiaomeng Liu, Hai Lin, and Ben M Chen. Structural controllability of switched linear systems. *Automatica*, 49(12):3531–3537, 2013.
- [17] Bin Meng. Observability conditions of switched linear singular systems. In *2006 Chinese Control Conference*, pages 1032–1037. IEEE, 2006.
- [18] B Molinari. Extended controllability and observability for linear systems. *IEEE Transactions on Automatic Control*, 21(1):136–137, 1976.
- [19] Sergio Pequito, Soumya Kar, and A Pedro Aguiar. A framework for structural input/output and control configuration selection in large-scale systems. *IEEE Transactions on Automatic Control*, 61(2):303–318, 2015.
- [20] Sérgio Pequito and George J Pappas. Structural minimum controllability problem for switched linear continuous-time systems. *Automatica*, 78:216–222, 2017.
- [21] Sérgio Pequito, Victor Preciado, and George J Pappas. Distributed leader selection. In *2015 54th IEEE Conference on Decision and Control (CDC)*, pages 962–967. IEEE, 2015.
- [22] Guilherme Ramos, A Pedro Aguiar, and Sergio Pequito. Structural systems theory: an overview of the last 15 years. *arXiv preprint arXiv:2008.11223*, 2020.
- [23] Guilherme Ramos, Sérgio Pequito, A Pedro Aguiar, and Soumya Kar. Analysis and design of electric power grids with p-robustness guarantees using a structural hybrid system approach. In *2015 European Control Conference (ECC)*, pages 3542–3547. IEEE, 2015.

- [24] Guilherme Ramos, Sérgio Pequito, A Pedro Aguiar, Jaime Ramos, and Soumya Kar. A model checking framework for linear time invariant switching systems using structural systems analysis. In *2013 51st Annual Allerton Conference on Communication, Control, and Computing (Allerton)*, pages 973–980. IEEE, 2013.
- [25] Guilherme Ramos, Sérgio Pequito, and Carlos Caleiro. The robust minimal controllability problem for switched linear continuous-time systems. In *2018 Annual American Control Conference (ACC)*, pages 210–215. IEEE, 2018.
- [26] Guilherme Ramos, Daniel Silvestre, and Carlos Silvestre. General resilient consensus algorithms. *International Journal of Control*, 0(ja):1–27, 2020.
- [27] Yuangong Sun, Yazhou Tian, and Xue-Jun Xie. Stabilization of positive switched linear systems and its application in consensus of multiagent systems. *IEEE Transactions on Automatic Control*, 62(12):6608–6613, 2017.
- [28] Shreyas Sundaram and Christoforos N Hadjicostis. Designing stable inverters and state observers for switched linear systems with unknown inputs. In *Proceedings of the 45th IEEE Conference on Decision and Control*, pages 4105–4110. IEEE, 2006.
- [29] Shreyas Sundaram and Christoforos N Hadjicostis. Structural controllability and observability of linear systems over finite fields with applications to multi-agent systems. *IEEE Transactions on Automatic Control*, 58(1):60–73, 2012.
- [30] Chun-Hua Xie and Guang-Hong Yang. Secure estimation for cyber-physical systems with adversarial attacks and unknown inputs: An l_2 -gain method. *International Journal of Robust and Nonlinear Control*, 28(6):2131–2143, 2018.